Climatology of Air Parcel Trajectories Related to the Atmospheric Transport of *Peronospora tabacina*

JERRY M. DAVIS, Department of Marine, Earth & Atmospheric Sciences and Department of Plant Pathology, and JOHN F. MONAHAN, Department of Statistics, North Carolina State University, Raleigh 27695

ABSTRACT

Davis, J. M., and Monahan, J. F. 1991. Climatology of air parcel trajectories related to the atmospheric transport of *Peronospora tabacina*. Plant Dis. 75:706-711.

Five years of temperature and wind data from atmospheric soundings were used in conjunction with the U.S. National Oceanic & Atmospheric Administration (NOAA) Air Resources Laboratories Atmospheric Transport and Dispersion (ATAD) model to construct an atmospheric air parcel trajectory climatology for the transport of the sporangiospores of the fungus *Peronospora tabacina*. With the receptor point in the North Carolina mountains, four receptor-oriented (backward-in-time) trajectories were calculated daily for April through August, as well as for the annual period. The 12-, 24-, and 48-hr air parcel positions, before the arrival of the air parcel in the mountains, were plotted. These spatial data were used in a nonparametric density estimation routine that generated plots of probability density function contours for the 12-, 24-, and 48-hr periods. Numerical integration was used to obtain probabilities from the contours of the probability density function. These analyses should be useful in assessing the probability that the specified location in western North Carolina received air parcels from various geographical locations; however, only those air parcels that come from regions where a source of diseased tobacco plants is present would be of epidemiological significance.

A number of recent papers have focused on the long-range atmospheric transport of the sporangiospores of *Peronospora tabacina* D. B. Adam, which causes blue mold of tobacco. Aylor et al (2) hypothesized that the blue mold epidemics that occurred in Connecticut in 1979 and 1980 resulted from windborne spores from sources hundreds of kilometers away. Davis and Main (5) examined the occurrence of blue mold in North Carolina in 1980. The importance of the atmospheric transport of spores in the geographical spread of the disease was documented. Davis and Main (6) and Davis et al (7) examined blue mold occurrences in central Kentucky in 1981 and 1982. Pathologists hypothesized that the source region for the inoculum was south-central Texas, where infected *Nicotiana repanda* Willd. ex Lehm. plants had been observed, rather than the more traditional source regions to the south and east of the disease outbreak sites. Atmospheric trajectory analysis provided support for south-central Texas as an inoculum source region. Subsequent work by Davis et al (8) focused on blue mold occurrence in central Kentucky in 1985. In this case, pathologists had information that allowed estimation of a narrow window-in-time for spore arrival at the leaf surface. The arrival time at the target area is a critical element in identifying inoculum source regions. Again, trajectory analysis provided support for an inoculum source region located in south-central Texas. In addition, the results of controlled environment research reported in Davis et al (8) indicated that the Texas region was capable of producing sufficient inoculum to reach the Kentucky outbreak site even with allowances made for dilution, deposition, and spore survival. Other aspects of modeling long-distance transport of spores are discussed in Davis (4).

The atmospheric transport process for fungal pathogens has many components including spore production, spore release from the plant, spore escape from the canopy into the lower atmosphere (the atmospheric boundary layer [ABL]), the mixing of the spores within the ABL, the transport of the spores within the ABL to distant locations, the survival of the airborne spores, and the deposition of the spores through both wet and dry deposition processes. The evidence for the long-range transport of spores is largely circumstantial in nature. Obtaining more substantial evidence would require large-scale ground-based and atmospheric-based sampling experiments. Also, the nature of the pathosystem itself presents a problem. *P. tabacina* is obligate and its sporangiospores can not easily be differentiated from other downy mildews. Short of extensive bioassays, it would be difficult to ascertain the specificity of the captured spore or to recognize it as the downy mildew that infects tobacco.

Circumstantial evidence for long-range spore transport involves certain characteristics of the disease cycle at both the inoculum source and at the new disease outbreak site. The atmospheric trajectory provides a logical spatial-temporal link between the inoculum source region (or potential regions) and new outbreak sites.

Given the numerous and costly problems that arise in conjunction with biological sampling, another approach has been considered. Aylor (1) provides a framework for modeling the entire transport process. The Aylor method was applied to the occurrence of blue mold in Kentucky in 1985 as discussed earlier and in Davis et al (8). It was shown that south-central Texas was a potential inoculum source region for the 1985 epidemic in Kentucky. If one accepts the hypothesis that long-range transport, short-range transport, or a combination of the two are critical in the annual blue mold epidemics, the determination of established as well as new source regions

The use of trade names in this publication does not imply endorsement by the North Carolina Agricultural Research Service nor criticism of similar ones not mentioned.

Accepted for publication 2 January 1991.

becomes important. In particular, for a specified disease outbreak site, what are the potential inoculum source regions, and what is the probability that the inoculum comes from each of these regions? For a specified disease outbreak site in the North Carolina mountains, this paper examines the degree to which various inoculum source regions play a role in providing spores to the new outbreak site.

MATERIALS AND METHODS

The relative importance of various inoculum source regions was assessed with the use of nonparametric density estimation and numerical integration procedures based on receptor-oriented air parcel trajectories for the period April to June for the years 1978 to 1982. In both 1979 and 1980, there were severe blue mold epidemics in the eastern United States. A point in the burley region of North Carolina served as the air parcel receptor point because of the variety of potential inoculum source regions within several days' travel. Spores arriving in the mountains could have taken many paths; however, there are three paths that appear to be most likely based on recent research (5). In one case, spores would come from infected *Nicotiana tabacum* L. plants in northern Florida or southern Georgia after having traversed Georgia and/or Alabama (5). Another path would bring the spores into the mountains from locations to the east (e.g., eastern North Carolina) (5). The third most likely path would bring spores from the west or southwest into the mountains.

Trajectory analysis. Trajectory calculations were made with the NOAA Air Resources Laboratories Atmospheric Transport and Dispersion (ATAD) model. The following description of the ATAD model was taken from Heffter (10), which should be consulted for additional details. Atmospheric boundary-layer trajectories were calculated with a meteorological data base that contains upper-air winds, temperatures, and heights from North American atmospheric sounding stations. The data for the model are available from near the surface to 500 mbar. The ATAD model calculates four trajectories a day beginning at 0000, 0600, 1200, and 1800 Greenwich mean time. An individual trajectory is composed of 40 3-hr time segments, yielding a total duration time of 5 days. The model can calculate both source-oriented (forward-in-time) and receptor-oriented (backward-in-time) trajectories. The calculations for each trajectory segment are based on an average wind in a transport layer, the depth of which is identified by the model using the vertical temperature profile in the lower atmosphere. For a more detailed discussion of the application of this model to problems in plant pathology, see Davis and Main (5,6).

Data for the trajectory climatology were obtained from the special ATAD data tapes (available from the U.S. National Climatic Data Center in Asheville, NC, as file NAMER-WINDTEMP). The terminal point for the trajectories was the U.S. Environmental Protection Agency Mountain Cloud Chemistry Program Site 1 located on Mt. Gibbs (lat. 35°44′05″ N, long. 82°17′15″ W) in Yancey County, which is a major producer of burley tobacco. The trajectories were calculated for air parcel positions 12, 24, and 48 hr before their arrival at the receptor point.

The annual maps of trajectory climatologies are based on calculations using data from 47 mo during the 5-yr period. Data for the other 13 mo were not available. Five years of data were available for each month through the period April to June. For July, 4 yr of data were available, whereas for August, only 3 yr of data could be obtained.

The receptor-oriented trajectories were terminated after having gone back 48 hr in time. This cutoff point was selected for atmospheric and biological reasons. Because of the complex nature of atmospheric motion patterns, trajectories that extend beyond about 48 hr tend to become unreliable. In addition, if the spores were being transported under essentially clear sky conditions, the proportion that would survive beyond 48 hr would be quite small because of the prolonged exposure to UV radiation. Aylor (1) points out that there is a clear need to quantify the spore survival rate in the atmospheric boundary layer for periods of 0.50–2.0 days.

Nonparametric density estimation. One can quantify the relative importance of an inoculum source region on a particular disease outbreak site by finding the spatial probability distribution of the previous positions occupied by air parcels that arrived at the outbreak site over

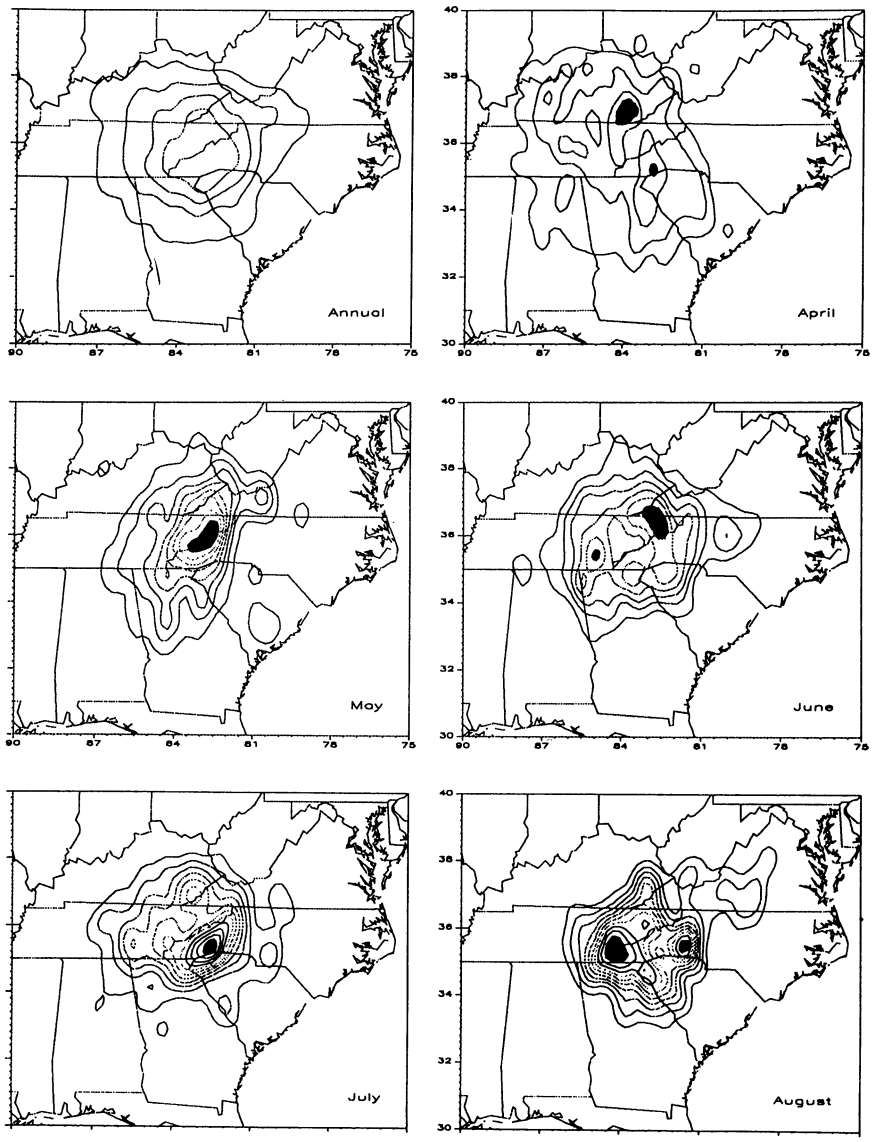

Fig. 1. Probability density function contour maps for air parcel positions 12 hr before arrival at the receptor point. Contour values start at 0.01 and continue in increments of 0.01. Higher values of the pdf have been shaded.

a specified time interval. The procedure used to quantify this relative importance is called nonparametric density estimation (NDE).

The ATAD model specifies air parcel trajectory positions by latitude and longitude, giving the location of an air parcel that arrives at a given location t time units later. Consider the two-dimensional sample space S of all possible positions (X,Y), the latitude/longitude pair, of such an air parcel. The long-term behavior of the air transport system with respect to a given location and time interval can be described by a bivariate probability density function (pdf), $f(x,y)$, over the two-dimensional space S, expressing relative frequencies of occurrence. Probabilities of a particular event, say the event A (where $A = [(x,y)\colon x_1 < x < x_2$ and $y_1 < y < y_2]$) can be computed by: $P(A) = \int_{y_1}^{y_2}\int_{x_1}^{x_2} f(x,y)\,dx\,dy$, giving the probability that an air parcel originated in a box-shaped area bounded by latitudes x_1 and x_2 and longitudes y_1 and y_2 and arrived at a given location t time units later.

This bivariate probability density function is not known in advance and must be estimated from the observations of positions $(X_i,Y_i) = 1,2,3,...n$. The NDE technique most commonly used is the kernel method, which can be viewed as smoothing the probability mass of each observation into a two-dimensional density, which is then summed over observations to produce the estimate. This estimate $\hat{f}$ can be written as: $\hat{f}(x,y) = (nh_xh_y)^{-1}\sum_{i=1}^{n} k[(x-X_i)/h_x, (y-Y_i)/h_y]$ where $k[(x-X_i)/h_x, (y-Y_i)/h_y]$ is called the kernel. Choosing k to be a bivariate density ensures that the estimate is not negative and integrates to one. The smoothing parameter h controls the spread of the probability mass around each observation (X_i,Y_i). Increasing h increases smoothing; decreasing h increases resolution, but taking h too small yields a ragged estimate. Another view of the kernel density estimate is that the spreading of the probability mass around each observation reflects the inherent inaccuracy of the trajectory positions produced by the transport model. In this sense, the contribution of each observation $k[(x-X_i)/h_x, (y-Y_i)/h_y]/(h_xh_y)$ describes a predictive distribution of the true source location of air parcel i. Increasing the smoothing parameter h reflects more uncertainty in the prediction.

For simplification and computational efficiencies in this work, the kernel k was chosen to be the product of two univariate densities, $k(u,v) = g(u)g(v)$, where $g(u)$ is the density of the sum of three variables with the uniform distribution: $g(u) = 0$ for $|u|>1$, $g(u) = (9/8)(1-3u^2)$ for $|u| < 1/3$, and $g(u) = (27/16)(|u| - 1)^2$ for $1/3 < |u| < 1$.

The figures in the Results section display contours of the estimated pdf $\hat{f}$. To obtain probabilities, one must integrate this pdf over the area of interest. The h values (in degrees) used were 0.8, 1.3, and 2.0 for the 12-, 24-, and 48-hr periods, respectively. The smoothing parameter h has been adjusted to account for the fact that the length of one degree of the meridian (110.953 km at about 36 N) differs from that of one degree of the parallel (90.168 km at about 36 N); hence, the use of h_x and h_y in the equations. This adjustment was made for the latitude and longitude of the receptor point (about 36 N, 82 W). The values selected for the smoothing parameters were chosen to reflect the inherent inaccuracies of the trajectory positions with time. A secondary criterion was the smoothness and visual appeal of the contour plots. Small changes in h did not yield any visual differences in the contour plots nor in the later probability calculations. The fact that the model-calculated trajectories are time dependent does not affect the plots of the pdf; however, the accuracy of the estimated pdf is affected. The result of this dependence is equivalent to reducing the number of observations by an amount based on the autocorrelation function for the time series involved.

Numerical integration. Numerical integration was used to compute the probabilities from the estimates of the pdf. Because the potential inoculum source region in northern Florida/southern Georgia is somewhat triangular in shape, a triangular version of Simpson's rule was employed. When integrating a function numerically on an interval, Simpson's rule can be viewed as a 2:1 weighted average of the midpoint rule and the trapezoid rule. In the triangular analogue, the midpoint rule would evaluate the function at the centroid of the triangle, where the medians meet; the trapezoid rule would use evaluations of the function at the vertices. The Simpson integration rule for the triangle would give the centroid point nine times that of a vertex and would give an exact result

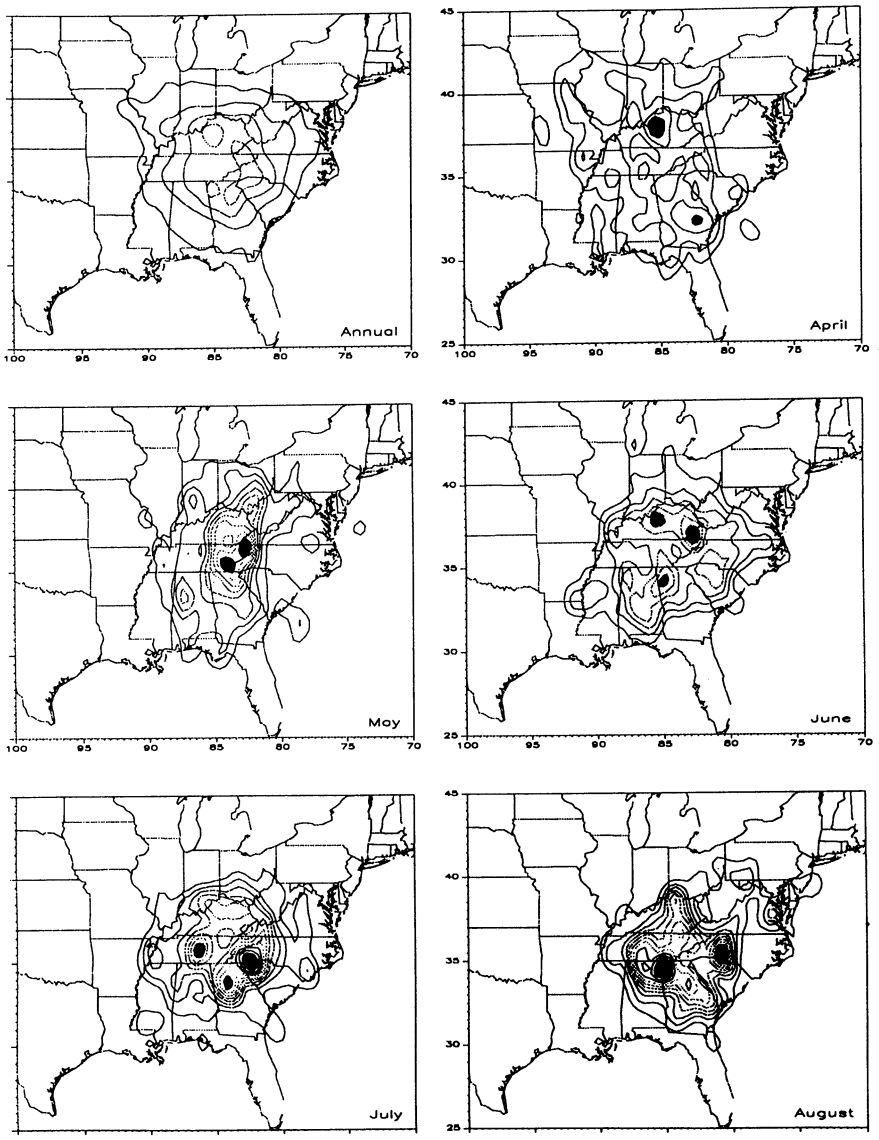

Fig. 2. Probability density function contour maps for air parcel positions 24 hr before arrival at the receptor point. Contour values start at 0.003 and continue in increments of 0.003. Higher values of the pdf have been shaded.

for a function of the form $f(x,y) = ax^2 + bxy + cy^2 + dx + ey + f$. In the case of this kernel density estimate, the pdf is piecewise cubic, so that the accuracy of this method using the smoothness of the function is difficult to assess. Following a brute-force approach, by subdividing each side 64 times, 4,096 (64^2) similar subtriangles are created, and the use of 6,241 function evaluations calculates the probabilities with an error less than 2×10^{-5}.

RESULTS

Figures 1–3 show the results of the pdf analysis. The calculations were based on an average atmospheric boundary-layer wind. Figure 1 shows the annual and monthly (April to August) trajectory climatologies for an air parcel 12 hr before its arrival at the receptor location. Figures 2 and 3 provide the same information for 24 and 48 hr before arrival at the receptor location, respectively. These months generally constitute the blue mold disease season. In this section of the mountains, tobacco seedlings are about 50–100 cm tall by mid-April, and approximately 50% of the tobacco acreage is transplanted by the first week in June.

The annual 12-hr map (Fig. 1A) shows nearly concentric contours around the receptor point. Air parcels are equally likely to come from any direction. The highest probabilities will be associated with those that travel short distances. In April (Fig. 1B), peaks in the pdf contours are located mainly to the north and south of the receptor site. Air parcels from these locations would still be traveling relatively short distances. In May (Fig. 1C), it is most likely that the parcel travels a short distance from the northwest to reach the receptor point. In June (Fig. 1D), it is most likely that the air parcel arrived at the receptor point from the north or west, while in July (Fig. 1E), the receptor point is located near the center of the highest contour value, indicating a short trip from a variety of locations. In August (Fig. 1F), air parcels would most likely travel a short distance from the west to reach the receptor site. A somewhat weaker peak is located to the east.

The annual plot (Fig. 2A) at 24 hr is again fairly concentric around the receptor site, although there is weak directional preference to the northwest and southwest. In April (Fig. 2B), peaks in the contours lie mainly to the south and north, whereas in May (Fig. 2C), air parcels, for the most part, would be required to travel short distances from the northwest to reach the receptor location. In June (Fig. 2D), directional preferences are to the southwest and to the northwest. In July (Fig. 2E), there is an area with a high pfd value that extends from the receptor site to the southwest. In addition, there is an isolated peak due west of the receptor site. In August (Fig. 2F), a high-valued pdf contour lies just to the east of the receptor site. Other peaks lie to the south, west, and northwest of the receptor site.

The annual pfd plot (Fig. 3A) for 48 hr shows weak directional preference to the northwest and southwest. Peaks in the contours for April (Fig. 3B) lie mainly to the north and south of the receptor site. These peaks are relatively weak. Peaks to the southwest and north characterize May (Fig. 3C). In June (Fig. 3D), the strongest peak lies over the northern Gulf of Mexico. In July (Fig. 3E), the strongest peaks lie to the south and west; however, there is another peak of significance to the north. Strong peaks lying to the southeast, southwest, and northwest dominate August (Fig. 3F).

An examination of the pdf contour plots in the broadest sense indicates agreement with basic wind field climatology. During the summer months, wind-field climatology indicates that the most frequently occurring wind directions are from the south, while in the winter months winds from the north predominate. Spring and fall months are the transition periods.

Figure 4A shows tobacco allotments by county in Alabama, Florida, and Georgia. The data were obtained from Flue-Cured Tobacco Allotted by Counties, 1989 (USDA Agricultural Stabilization and Conservation Service, Commodity Analysis Division). A triangle was used to enclose these counties, including a few counties without an allotment. Using the numerical integration procedures outlined earlier, the probability was obtained by integrating over the pdf for the triangular area. The results of this integration are shown in Table 1. The numbers in the body of the table are the probabilities (by month and annual period) that an air parcel was residing in the triangular area in Figure

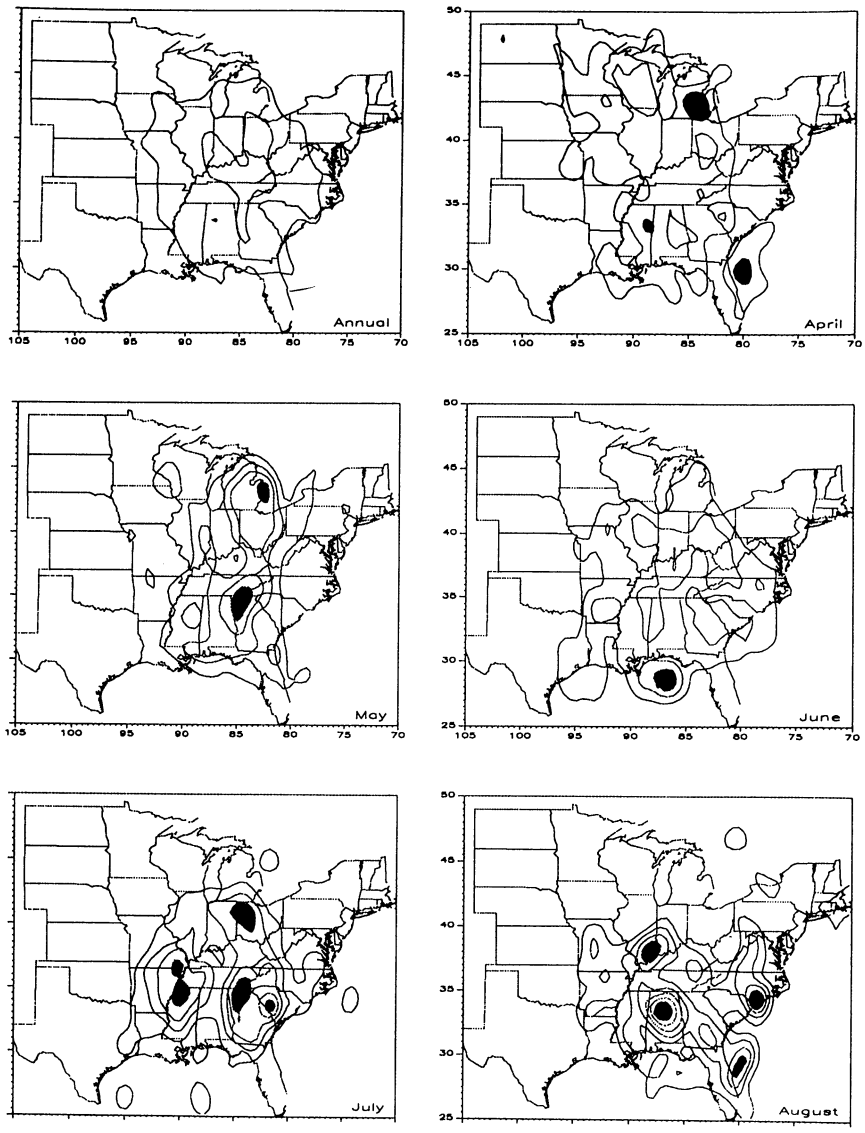

Fig. 3. Probability density function contour maps for air parcel positions 48 hr before arrival at the receptor point. Contour values start at 0.002 and continue in increments of 0.002. Higher values of the pdf have been shaded.

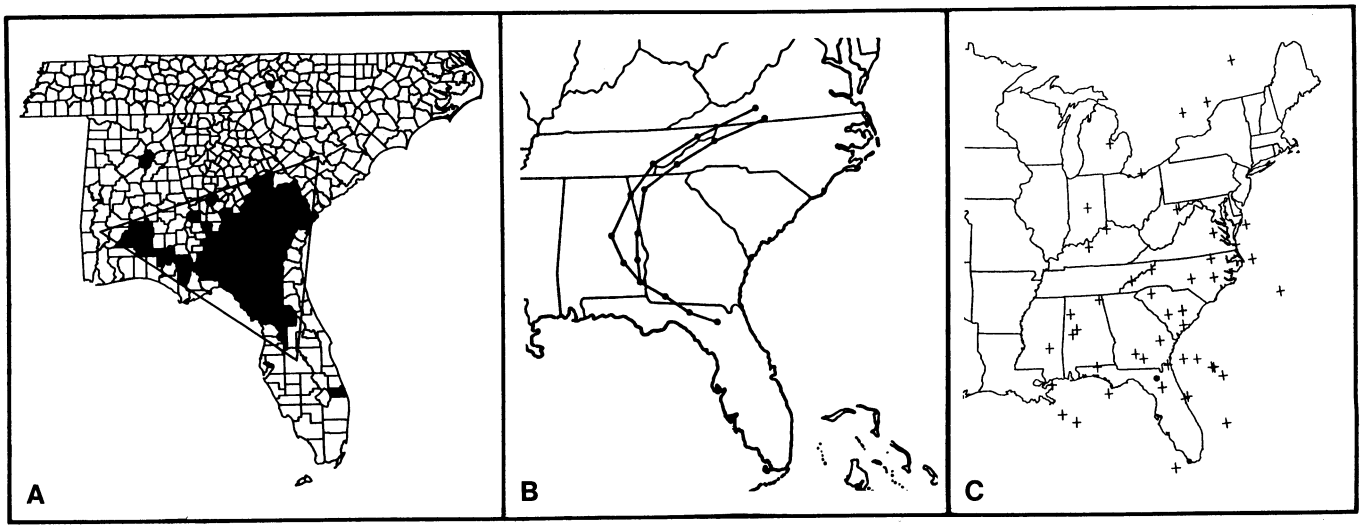

Fig. 4. (A) Flue-cured tobacco allottments by counties in Florida, Georgia, and Alabama. Triangle indicates area over which the probability density function was integrated. The dot in the mountains of North Carolina indicates the receptor point. **(B)** An example of an ATAD model forward trajectory from the tobacco production area in northern Florida/southern Georgia to the mountains of North Carolina. The trajectory on the left departed the source region at 0700 EST on 29 May 1980, while the one on the right departed the source region at 1300 EST on 29 May 1980. Reprinted with permission from Davis (4). **(C)** ATAD model calculations of air parcel positions 48 hr after leaving northern Florida at 1300 EST on each day during April–June 1980. The origin point for the source-oriented trajectories is indicated by the dot in northern Florida. Reprinted with permission from Davis (5).

Table 1. Probability (by month and annual period) that an air parcel resided in the tobacco production area[a] 12, 24, or 48 hr before arrival at the specified disease outbreak site in the North Carolina mountains

Time	12-hr period	24-hr period	48-hr period
Annual	0.044	0.070	0.053
April	0.062	0.120	0.039
May	0.034	0.082	0.074
June	0.008	0.051	0.043
July	0.020	0.040	0.084
August	0.006	0.105	0.083

[a] In northern Florida/southern Georgia (Fig. 4A).

4A 12, 24, or 48 hr before arrival at the designated receptor point. Table 1 shows that the probabilities at the 12-hr time slot tend to be smaller than those for the other time periods. This result is to be expected because it is not likely that an air parcel will make a trip of that length in 12 hr (Fig. 1). April and August provide the highest probabilities for the 24-hr period, while May, July, and August dominate the 48-hr period (Figs. 2 and 3).

The nonparametric density estimation procedure provides a visually appealing view of the spore dispersion patterns. For computing the probability of an air parcel arising from the triangular region, an alternative method would be the proportion leaving the triangle. For example, for the annual 12-hr period, the probability computed in this manner is 0.042, whereas the integrated value is 0.044.

Figure 4B shows typical ATAD trajectories from the triangular region to the mountains of North Carolina for 29 May 1980. Figure 4C shows ATAD calculated air parcel positions 48 hr after leaving a specific point in the triangular region for the period April–June 1980. Clearly, air parcels move off in many directions from the source region.

Because the original pdf and probability calculations were based on four ATAD trajectories per day (the model default procedure), Table 1 can be used to estimate the probability that at least one of these four air parcels was residing in the triangular area 12, 24, or 48 hr before arriving at the receptor point. For example, for the 48-hr time slot, this probability can be obtained from P (at least one of the four parcels residing in the triangular area 48 hr before arriving at the receptor site) $= 1 - P$ (none of the four reside in the triangular area 48 hr before arriving at the receptor site).

For example, for a day in August at the 48-hr time slot, the probability of an air parcel residing in the triangular area 48 hr before arrival at the receptor point is 0.083. Thus, the P (at least one) $= 1 - (0.917)^4 = 0.29$. The probabilities are estimates because the individual events, i.e., the trajectory of an air parcel, are not independent of each other.

It is important to note that the probability calculation above is based on the four-per-day model-generated trajectories. In actual practice, the movement of air parcels from a source region to a receptor point is much more episodic in nature. On a climatological basis, atmospheric circulation regimes favor south-to-north transport during the spring to fall time period in the Southeast. Within this broad period, transport events are usually episodic. A short duration circulation event may favor the repeated transport of air parcels from the triangular region to the receptor point over several days. Thus, providing inoculum is present, it is quite likely that the receptor point will receive spores. For other periods, the winds may be completely unfavorable for any transport from the triangular region to the receptor point.

Figure 3 indicates that the probability that an air parcel reaches the receptor point from as far away as south-central Texas in 48 hr is very small. However, this region should not be ruled out as a potential inoculum source region. If synoptic-scale weather patterns favoring transport between these regions were to persist over many days, many air parcels might make such a trip, thereby increasing the the likelihood of significant spore transport, provided the inoculum was present in Texas and the survival rate was favorable.

DISCUSSION

The probability that an air parcel traveled from any given potential inoculum source region to the receptor point in the mountains can be obtained in a manner similar to that outlined earlier. Receptor-oriented climatologies can also be derived for other receptor points. In addition, source-oriented climatologies can be constructed. Recall that the crosses in Figure 4C indicate the positions of air parcels 48 hr after leaving a point within the triangle shown in Figure 4A for the period April–June 1980. These

model calculations could be extended in time to include additional months and years. These data could then be used to calculate the pdf from which probabilities could be extracted by integrating the pdf over the desired geographical region. For an air parcel that departed the selected inoculum source region, one could calculate the probability it would reside in a given geographical region 12, 24, or 48 hr later.

Both the source- and receptor-oriented climatologies serve as planning tools for disease management decisions. Real-time forecasts of the movement of air parcels can readily be obtained by combining a numerical weather prediction model with a long-range transport model. The Nested Grid model, which is a numerical weather prediction model, provides 12-, 24-, 36-, and 48-hr forecasts for the atmospheric boundary-layer winds. These grid-point wind forecasts, along with any other pertinent model output data, could be used in conjunction with a long-range transport model to provide real-time forecasts of air parcel positions subsequent to departure from a potential inoculum source region. This linked-model approach has been in operation for many years to trace the movement of hazardous materials that are accidentally released into the atmosphere.

The weak point in both the climatologies and the real-time forecasts lies in not knowing if the air parcels contain viable spores. On-site inspection at the source region can determine if inoculum is being produced; however, the level of production is harder to ascertain. The greater the spore production at the source, the greater the chances that spores will find their way to distant receptor sites, all other factors being the same. If the spore production rate is known or can be estimated, most long-range transport models provide estimates of deposition along the air parcel path. Some of the more recent models make an effort to handle the diurnal changes in the structure of the atmospheric boundary layer in a realistic manner. A description of these diurnal changes can be found in Davis (4).

Alternately, similar calculations can be made by a personal computer or by hand with the framework provided by Aylor (1). The Aylor model has been applied to spore transport from south-central Texas to Kentucky by Davis et al (8). The Aylor model is essentially a one-layer model that does not specifically take into account the aforementioned diurnal changes in the structure of the boundary layer. At night, portions of the daytime spore cloud at one level in the atmosphere can move in a direction and speed that is quite different from the movement experienced by spores at other levels (12,13). On the other hand, the Aylor model provides an excellent means to get a sound estimate of the number of viable spores arriving at a distant potential disease outbreak site. This approach will be used to get such estimates for the triangular area shown in Figure 4A. In the application of the model, many of the parameter values were taken from Aylor (1).

The two basic equations in the Aylor model are: $D = v_d PFETS$ and $D_T = \int_0^\infty D dt$. In the first equation, v_d is dry deposition velocity (0.01 $m \cdot s^{-1}$); P is the daily spore production from a 500-ha field of diseased tobacco (6.44×10^{13} spores per day); F is the fraction of the daily production of spores released during an event centered at 1000 hr (0.33); E is the fraction of the spores that leave the tobacco leaf canopy and enter the lower atmosphere (0.15); T is a transport function (6.5×10^{-14} m^{-3}) that includes the effects of dilution that arise from turbulent mixing in the atmosphere and from vertical shear in the horizontal wind speed and direction and ground deposition of spores along the transport route; and S is the fraction of the spores that survive the trip (different values will be used). S is based on the exposure time of the spores to solar radiation.

To obtain T, the across-wind standard deviation of the spore cloud (σ_y) must be be specified. Aylor uses the empirical equation suggested by Heffter (10,11), $\sigma_y = 0.5t$, where σ_y is in meters and t is in seconds. Observational evidence (9) from long-range plume dispersion measurements indicates that the Heffter equation is adequate for use in the present case. It is also common to assume that the down-wind standard deviation of the spore cloud (σ_x) equals the across-wind value. The calculation of T also requires an estimate of the height of the atmospheric boundary layer. During the day, the convective boundary layer is generally between 1 and 2 km high, while at night the height of the stable boundary layer is typically about 100 m. A height of 1.5 km was used for the convective boundary layer. A transport layer wind is also required to estimate T. A good approximation to the transport-layer wind is the surface geostrophic wind, which can be obtained from the surface wind data following a procedure outlined by Danard (3). Following this method yields a transport-layer wind of about 30 km hr^{-1}.

For an S value of 0.1 (roughly characteristic of overcast conditions), about two spores per square meter would be deposited on potential disease outbreak sites in the mountains of North Carolina; for an S value of 0.01 (characteristic of partly cloudy conditions), the number would be two spores per 10 m^2; and for an S value of 0.001 (characteristic of clear sky conditions) about two spores per 100 m^2 would be deposited. In each case, it was assumed that the spores were exposed to 8 hr of day transport and 12 hr of night transport. Thus, sensitivity to exposure to solar radiation can be a dominating factor. Transport from south to north in the Southeast United States usually takes place on the backside of a high-pressure system where conditions are usually partly cloudy. Again, if transport-level winds remained favorable over several days, many viable spores might be transported to fields in the mountains.

ACKNOWLEDGMENTS

Support for this research was provided by R. J. Reynolds, Inc. and the North Carolina Tobacco Foundation. We thank Paul Marsh (Department of Statistics, NCSU) and Steven Seabaugh for preparing the probability density function plots, H. A. Devine (College of Forest Resources, NCSU) for the preparation of the triangular area shown in Figure 4A, and C. E. Main (Department of Plant Pathology, NCSU) for his many helpful comments on the manuscript.

LITERATURE CITED

1. Aylor, D. E. 1986. A framework for examining inter-regional aerial transport of fungal spores. Agric. For. Meteorol. 38:263-288.
2. Aylor, D. E., Taylor, G. E., and Raynor, G. S. 1982. Long-range transport of tobacco blue mold spores. Agric. Meteorol. 28:217-232.
3. Danard, M. 1988. A diagnostic method for computing the surface wind from the geostrophic wind including the effects of baroclinity. Mon. Weather Rev. 116:2712-2716.
4. Davis, J. M. 1987. Modeling the long-range transport of plant pathogens in the atmosphere. Annu. Rev. Phytopathol. 25:169-188.
5. Davis, J. M., and Main, C. E. 1984. A regional analysis of the meteorological aspects of the spread and development of blue mold on tobacco. Boundary-Layer Meteorol. 28:271-304.
6. Davis, J. M., and Main, C. E. 1986. Applying atmospheric trajectory analysis to problems in epidemiology. Plant Dis. 70:490-497.
7. Davis, J. M., Main, C. E., and Nesmith, W. C. 1985. The biometeorology of blue mold of tobacco. Part II: The evidence for long-range sporiangospore transport. Pages 473-498 in: The Movement and Dispersal of Agriculturally Important Biotic Agents. D. R. MacKenzie, C. S. Barfield, G. C. Kennedy, and R. D. Berger, eds. Claitor's Publishing Division, Inc., Baton Rouge, LA.
8. Davis, J. M., Main, C. E., and Nesmith, W. C. 1989. The aerobiological aspects of the occurrence of blue mold in Kentucky in 1985. Pages 55-71 in: Blue Mold Diseases of Tobacco. C. E. Main and H. W. Spurr, eds. Proc. Symp. Blue Mold Dis. Tob.
9. Gifford, F. A. 1982. Long-range dispersion: Comparisons of the Mt. Isa data with theoretical and empirical formulas. Atmos. Environ. 16:1583-1586.
10. Heffter, J. L. 1980. Air Resources Laboratories Atmospheric Transport and Dispersion Model (ARL-ATAD). NOAA Tech. Mem. ERL ARL-81. National Oceanic & Atmospheric Administration, Silver Spring, MD. 17 pp.
11. Heffter, J. L. 1983. Branching Atmospheric Trajectory (BAT) Model. NOAA Tech. Mem. ERL ARL-121. National Oceanic & Atmospheric Administration, Silver Spring, MD. 16 pp.
12. Venkatram, A. 1988. Dispersion in the stable boundary layer. Pages 229-265 in: Lectures on Air Pollution Modeling. A. Venkatram and J. C. Wyngaard, eds. American Meteorological Society, Boston, MA.
13. Weil, J. C. 1988. Dispersion in the convective boundary layer. Pages 167-227 in: Lectures on Air Pollution Modeling. A. Venkatram and J. C. Wyngaard, eds. American Meteorological Society, Boston, MA.